Solution 1 – parts a to d

a)

Photon angular frequency = ω_p

$\therefore$ Energy of photon = $E_p = \hbar\omega_p$.

Absorbtion of the photon excites a valance band electron into the conduction band. This requires conservation of energy and momentum. As Si is an indirect bandgap semiconductor a phonon is necessary to allow conservation of momentum:-

Conservation of momentum $\Rightarrow$

$\hbar k_e = \hbar k_h + \hbar q$ where k_e = conduction band electron wavevector.

k_h = valance band hole wavevector.

q = phonon wavevector.

Conservation of energy $\Rightarrow$

$\hbar\omega_p = E_g - \hbar\omega_q$ where ω_q = Ang frequency of phonon. [3]

As a phonon is necessary for the process to occur, the overall probability is Low $\Rightarrow$ Si is optically inactive.

In a Si nanocrystal, momentum conservation is not a restriction. This is because, from Heisenberg's uncertainty principle, $\Delta p \Delta x \geq \frac{\hbar}{2}$, as Δx is very small (~ nanocrystal size), Δp is large and an additional phonon is not necessary. Therefore, a Si nanocrystal is optically active. [2]

b) (i) The given 2s state is symmetric, and the three 2p states are aligned along x, y, and z axis:

1. Symmetric:

$$|2s\rangle = \psi_{200} \sim \left(1 - \frac{Zr}{2a_0}\right) e^{-\frac{Zr}{2a_0}}$$

2. Aligned along x, y, and z axis:

$$|2p_x\rangle \sim xe^{-\frac{Zr}{2a_0}} \qquad |2p_y\rangle \sim ye^{-\frac{Zr}{2a_0}} \qquad |2p_z\rangle \sim ze^{-\frac{Zr}{2a_0}}$$

For each sp^2 'σ'orbital, we require the 2s state, and two 2p states. Furthermore, if one sp^2 orbital is aligned with the $+x$-axis, then the others need to be 60° above and below the $-x$ axis. This gives the required 120° separation between the three sp^2 orbitals.

In view of this, we may construct linear combinations for the sp^2 orbitals as follows:

$$|sp_1^2\rangle = |2s\rangle + \sqrt{2}|2p_x\rangle$$

$$|sp_2^2\rangle = |2s\rangle + \sqrt{\frac{3}{2}}|2p_y\rangle - \sqrt{\frac{1}{2}}|2p_x\rangle$$

$$|sp_3^2\rangle = |2s\rangle - \sqrt{\frac{3}{2}}|2p_y\rangle - \sqrt{\frac{1}{2}}|2p_x\rangle$$

[3]

(ii) Sketches for σ and π orbitals along a hexagonal ring:

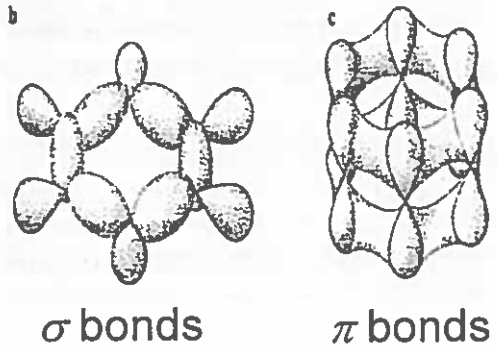

[2]

c) The vapour-liquid-solid (VLS) growth mechanism uses metal nanoparticles (typically Au or Fe) as a catalyst to grow Si nanowires. The wires may be grown by CVD, or PECVD, from SiH_4 gas, in the presence of Au nanoparticles on a substrate. The Au-Si phase diagram is shown below (this may be shown schematically):

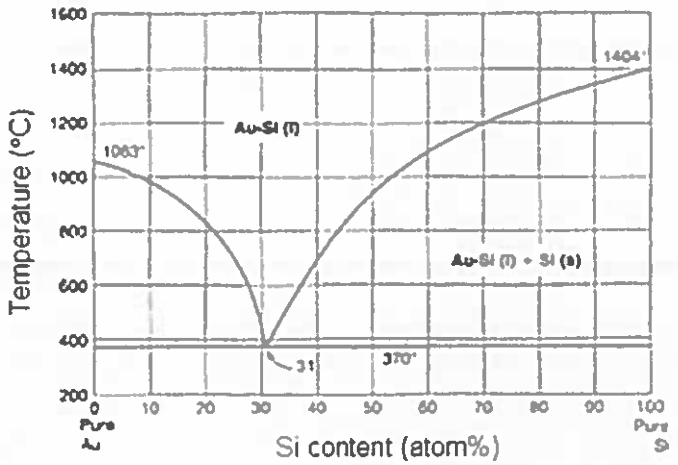

The phase diagram predicts that Au nanoparticles would form a liquid Au-Si alloy at temperature $T > 363°C$ (Eutectic point). For this temperature range, during the CVD/PECVD process, super-saturation of Si in the nanoparticle alloy leads to precipitation of solid Si and the formation of a solid Si/liquid Si/Au-Si alloy interface. Subsequent growth of a 1-D Si nanowire occurs from this interface. The process is shown schematically in the figure below:

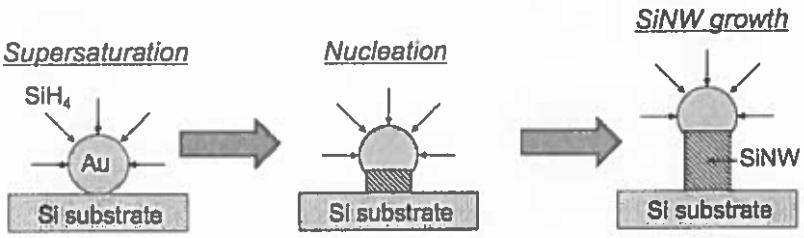

[4]

d) The Chiral vector C_h may be constructed using the fundamental translational vectors a_1 and a_2 using $C_h = na_1 + ma_2$. This gives for vectors X, Y and Z the following values of (n, m):

$X = 3a_1 + 3a_2 \Rightarrow (n_X, m_X) = (3, 3)$
$Y = 6a_1 + 3a_2 \Rightarrow (n_Y, m_Y) = (6, 3)$
$Z = 5a_1 + a_2 \Rightarrow (n_Z, m_Z) = (5, 1)$

[3]

X is then a Chiral vector with $n = m$, implying an 'armchair', metallic nanotube.

Y is then a Chiral vector with $n - m = 3 = 3j$, where the integer $j = 1$. This implies a semiconducting nanotube with a small band gap E_g.

Z is then a Chiral vector with $n - m = 4 = 3j + 1$, where the integer $j = 1$. This again implies a semiconducting nanotube, but in this case with a large band gap E_g.

[3]

go to p 10 .

Solution 2

(a) We scale the device dimensions by a factor k, such that t_{ox}, L, and W change to t_{ox}/k, L/k, and W/k.

[2]

In order to keep electric fields F constant, the following changes must be made:

(i) Doping concentration:

In the channel region, Poisson's Eq. $\Rightarrow \frac{\partial F_x}{\partial x}+\frac{\partial F_y}{\partial y}=\frac{-eN_A}{\varepsilon_{Si}\varepsilon_o}$

So, to keep F_x, F_y constant when dimensions are scaled by $1/k$, we must scale N_A and N_D by k: $\Rightarrow N_A, N_D \rightarrow kN_A, kN_D$

[4]

(ii) Voltages:

As $F \sim V/L$, reducing L by $L/k \Rightarrow V \rightarrow V/k$.

[2]

(iii) Gate capacitance:

As $C = \varepsilon_{ox}\varepsilon_O A/t_{ox}$, and $A \rightarrow A/k^2$, $t_{ox} \rightarrow t_{ox}/k \Rightarrow C \rightarrow C/k$.

[4]

(iv) Inversion layer charge density:

$Q_n \sim CV/A$ and $C \rightarrow C/k$, $V \rightarrow V/k$, $A \rightarrow A/k^2$. This $\Rightarrow Q_n$ remains constant.

[2]

(b) For the saturation and sub-threshold currents:

(i) Drift current (linear and saturation region current):

$I_{drift}/W = Q_n v$, where $v = \mu F$ is the carrier velocity. As both Q_n and v are constant, $\Rightarrow I_{drift}/W$ remains constant.

But, as $W \rightarrow W/k$, we have $I_{drift} \rightarrow I_{drift}/k$

[4]

(ii) Diffusion current (sub-threshold current):

$I_{diff} / W = D_n(dQ_n /dx) = (mkT/e)(dQ_n /dx)$. As Q_n is constant, and $x \rightarrow x/k$, $\Rightarrow I_{diff}/W \rightarrow k(I_{diff}/W)$, i.e. I_{diff}/W increases by a factor k. But, as $W \rightarrow W/k$, we find I_{diff} is constant.

[4]

(c) [This part needed generalised scaling, not considered in detail in the course. However, candidates should be able to apply the techniques used in parts a and b to solve this part].

Again, consider Poisson's equation in the channel region:

$$\frac{\partial F_x}{\partial x} + \frac{\partial F_y}{\partial y} = \frac{-eN_A}{\varepsilon_{Si}\varepsilon_o}$$

Here, reducing $L \rightarrow L/k$ but $N_A \rightarrow \alpha N_A \Rightarrow F \rightarrow \alpha F$.

Hence, as $F \sim V/L$, reducing L by $L/k \Rightarrow V \rightarrow \alpha V/k$, $\Rightarrow \sigma = \alpha/k$

[4]

Gate capacitance $C = \varepsilon_{ox}\varepsilon_O A/t_{ox}$, depends only on device dimensions, hence this scales as before, $C \rightarrow C/k$.

We may then find the effect on the inversion layer charge density:

$Q_n \sim CV/A$ and $C \rightarrow C/k$, $V \rightarrow \alpha V/k$, $A \rightarrow A/k^2$. This $\Rightarrow Q_n \rightarrow \alpha Q_n$.

[4]

Solution 3

a) [This question follows a normalisation question in a problem sheet in the course]

$$\psi = A\exp\left(\frac{-Zr}{a_0}\right)$$

Normalising in spherical coordinates:

$$\int_{r=0}^{\infty}\int_{\theta=0}^{\pi}\int_{\phi=0}^{2\pi}\psi_{100}^2\, r^2 \sin\theta\, dr\, d\theta\, d\phi = 1$$

$$\Rightarrow A^2\int_0^{\infty}\int_0^{\pi}\int_0^{2\pi} e^{\frac{-2Zr}{a_0}} r^2\sin\theta\, dr\, d\theta\, d\phi \qquad [2]$$

$$= A^2\int_0^{\infty} e^{\frac{-2Zr}{a_0}} r^2\, dr \int_0^{\pi}\sin\theta\, d\theta \int_0^{2\pi} d\phi$$

$$= A^2\left|-\cos\theta\right|_0^{\pi}\cdot\left|\phi\right|_0^{2\pi}\cdot\left(\left|\frac{r^2 e^{-2Zr/a_0}}{\frac{-2Z}{a_0}}\right|_0^{\infty} - \int_0^{\infty}\frac{2r\, e^{\frac{-2Zr}{a_0}}}{\frac{-2Z}{a_0}}dr\right) \qquad [4]$$

$$= -A^2(-1-1)\cdot(2\pi-0)\cdot\left(+\frac{2a_0}{2Z}\int_0^{\infty} r e^{\frac{-2Zr}{a_0}}dr\right)$$

$$= +8\pi A^2\left(\frac{a_0}{2Z}\left(\left|\frac{r\, e^{-2Zr/a_0}}{\frac{-2Z}{a_0}}\right|_0^{\infty} - \int_0^{\infty}\frac{e^{-2Zr/a_0}}{\frac{-2Z}{a_0}}dr\right)\right)$$

$$= +8\pi A^2\left(\frac{a_0}{2Z}\left(+\frac{a_0}{2Z}\left|\frac{e^{\frac{-2Zr}{a_0}}}{\frac{-2Z}{a_0}}\right|_0^{\infty}\right)\right)$$

$$= +8\pi A^2\left(\frac{a_0}{2Z}\right)^2\cdot\left(-\frac{a_0}{2Z}(0-1)\right)$$

$$= +8\pi A^2\left(\frac{a_0}{2Z}\right)^3 = 1$$

$$\Rightarrow \quad A = \sqrt{\frac{1}{\pi}}\left(\frac{Z}{a_0}\right)^{3/2} \qquad [4]$$

b) [This question requires solving Schrödinger Equation in three dimensions, for both particle energies and wave functions].

(i) Schrödinger's Equation in 3-D is:-

$$\frac{-\hbar^2}{2m}\nabla^2\psi + V\psi = E\psi$$

If ψ is separable, we have $\psi = u(x)v(y)w(z)$

$E = E_x + E_y + E_z$

$V = V_x + V_y + V_z$ [2]

Substituting $\Rightarrow$

$$\frac{-\hbar^2}{2m}\left(\frac{d^2}{dx^2}+\frac{d^2}{dy^2}+\frac{d^2}{dz^2}\right)uvw + (V_x+V_y+V_z)uvw = (E_x+E_y+E_z)uvw$$

$$\Rightarrow \frac{-\hbar^2}{2m}\left(vw\frac{d^2u}{dx^2}+uw\frac{d^2v}{dy^2}+uv\frac{d^2w}{dz^2}\right)+(V_x+V_y+V_z)uvw = (E_x+E_y+E_z)uvw$$

$$\Rightarrow \frac{-\hbar^2}{2m}\left(\frac{1}{u}\frac{d^2u}{dx^2}+\frac{1}{v}\frac{d^2v}{dy^2}+\frac{1}{w}\frac{d^2w}{dz^2}\right)+(V_x+V_y+V_z)=E_x+E_y+E_z$$ [3]

$$\Rightarrow \frac{-\hbar^2}{2m}\frac{d^2u}{dx^2}+(V_x-E_x)u=0$$

$$\frac{-\hbar^2}{2m}\frac{d^2v}{dy^2}+(V_y-E_y)v=0$$

$$\frac{-\hbar^2}{2m}\frac{d^2w}{dz^2}+(V_z-E_z)w=0$$

These are three 1-D Schrödinger Equations

[3]

(ii) For all three directions x, y, z, V is zero within the well. The problem then reduces to three 1-D solutions, e.g.

For x-direction:

$$\frac{-\hbar^2}{2m}\frac{d^2u}{dx^2}+(V_x-E_x)u=0$$

Within the well, $0<x<L_x$, $V_x=0$

$$\Rightarrow \frac{-\hbar^2}{2m}\frac{d^2u}{dx^2}-E_xu=0$$

This has a general solution of the form:

$u = A\sin k_x x + B\cos k_x x$ where $k_x = \sqrt{\frac{2mE_x}{\hbar^2}}$ [2]

Substituting boundary conditions $u=0$ at $x=0$

$\Rightarrow B = 0 \Rightarrow u = A\sin k_x x$

Substituting $u=0$ at $x = L_x$

$\Rightarrow 0 = A\sin k_x L_x \Rightarrow k_x L_x = n\pi$, $n = 1,2,\ldots$

$\Rightarrow E_n = \frac{\hbar^2 k_x^2}{2m} = \frac{n^2\pi^2\hbar^2}{2mL_x^2}$

Similarly, $E_g = \frac{g^2\pi^2\hbar^2}{2mL_y^2}$ for y-direction, $g = 1,2,\ldots$

$E_l = \frac{l^2\pi^2\hbar^2}{2mL_z^2}$ for z-direction, $l = 1,2,\ldots$

$\therefore E_{ngl} = E_n + E_g + E_l = \frac{\pi^2\hbar^2}{2m}\left(\frac{n^2}{L_x^2} + \frac{g^2}{L_y^2} + \frac{l^2}{L_z^2}\right)$ [4]

Full wavefunction $\psi = uvw = A_x A_y A_z \sin k_x x . \sin k_y y . \sin k_z z$

$= C \sin k_x x . \sin k_y y . \sin k_z z .$

where $k_x = \frac{n\pi}{L_x}$, $k_y = \frac{g\pi}{L_y}$, $k_z = \frac{l\pi}{L_z}$

Normalising: $\int_0^{L_x}\int_0^{L_y}\int_0^{L_z} C^2 \sin^2 k_x x \sin^2 k_y y \sin^2 k_z z \, dx\,dy\,dz = 1$ [2]

$\Rightarrow C^2 \int_0^{L_x} \sin^2 k_x x\,dx \int_0^{L_y} \sin^2 k_y y\,dy \int_0^{L_z} \sin^2 k_z z\,dz = 1$

$\Rightarrow C^2 \int_0^{L_x}\left(\frac{1-\cos 2k_x x}{2}\right)dx \int_0^{L_y}\left(\frac{1-\cos 2k_y y}{2}\right)dy \int_0^{L_z}\left(\frac{1-\cos 2k_z z}{2}\right)dz = 1$

$\Rightarrow C^2\left(\frac{L_x}{2}\right)\left(\frac{L_y}{2}\right)\left(\frac{L_z}{2}\right) = 1 \Rightarrow C = \sqrt{\frac{8}{L_x L_y L_z}}$

$\therefore \psi_{ngl} = \sqrt{\frac{8}{L_x L_y L_z}} \sin\frac{n\pi}{L_x} \sin\frac{g\pi}{L_y} \sin\frac{l\pi}{L_z}$

[4]

Solution 1 – parts e to h

e) The force due to each actuator is:

$$F_0 = \frac{N\varepsilon_0 h}{2g} V_0^2$$

where N is the number of electrode gaps, h is the electrode depth, g is the inter-electrode gap and V_0 is the applied voltage. This result can be quoted if known or derived by virtual work. When the resonator is driven differentially by anti-phase square waves switching between zero and V_0, the driving force will be a zero-average square wave with amplitude F_0. Because the Q is relatively high, the response at resonance will be dominated by the fundamental component of the driving force which has amplitude $4F_0/\pi$. The resonant oscillation will then have amplitude $A_0 = 4QF_0/(\pi k)$ where k is the spring constant.

Putting $N = 198$, $h = 15$ μm, $g = 2$ μm, $V_0 = 5$ V we find $F_0 = 0.164$ μN. With $Q = 100$ and $k = 10$ N/m, the corresponding resonant oscillation amplitude is $A_0 = 2.1$ μm or 4.2 μm pk-pk. [5]

f) Typical structure of a shape bimorph actuator:

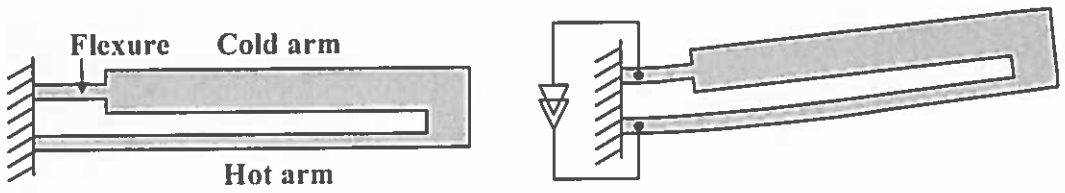

(i) The structure deflects to allow differential expansion of the hot and cold arms. Assuming all the heating occurs in the hot arm, the length mis-match will be $\sim\alpha L_h \Delta T$ where L_h is the length of the hot arm and ΔT is its average temperature rise. This must be equal to $g\theta$, where θ is the (small) angular deflection and g is the gap between the beams. Assuming the flexure (length L_f) bends as a circular arc, and the cold arm (L_c) remains straight, the tip deflection will be:

$$v \approx (L_c + L_f/2)\theta \approx L_h\theta \approx \alpha L_h^2 \Delta T / g \qquad [3]$$

(ii) The force required to hold the actuator at zero deflection is obtained by taking moments which gives $F = Rg/L_h$ where R is the axial reaction force at the supports. The reaction is equal to the axial elastic force due to the frustrated thermal expansion of the hot arm. Since virtually all the strain is in the hot arm, we have $R \approx EA\alpha\Delta T$ where A is the hot arm cross-section. We can therefore express F as:

$$F \approx \alpha EA\Delta T g/L_h \qquad [2]$$

Useful diagrams (not required):

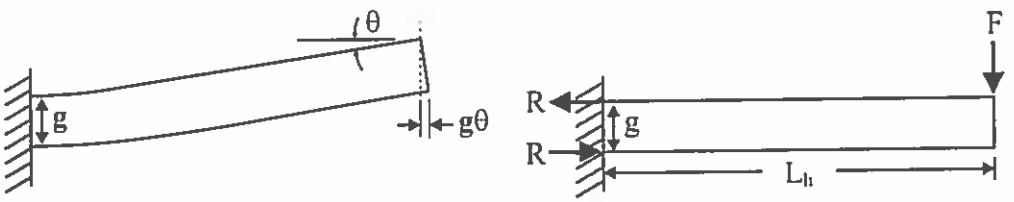

g) A grating of period d will generate diffracted beams at angles θ_n given by the Bragg condition:

$$\sin\theta_n = n\frac{\lambda}{d} \qquad n = 0, \pm 1, \pm 2 \ldots$$

The finest grating that will be resolved is the one for which the ±1 diffraction orders just pass through the projection lens. In this case we have $\theta_1 = \theta_m$ where θ_m is the maximum acceptance angle of the lens. But $\sin\theta_m = NA_o$ where NA_o is the numerical aperture on the object side, so for the finest resolvable grating we have:

$$d_{\min} = \frac{\lambda}{NA_o}$$

and the minimum resolvable half-pitch on the object side is:

$$R_o = \frac{d_{\min}}{2} = \frac{\lambda}{2NA_o}$$

The corresponding half-pitch on the image side is $R = R_o/m$, where m is the magnification, while the image side numerical aperture is $NA = mNA_o$, so we can recast the above formula for the image side as:

$$R = \frac{\lambda}{2NA}$$

[5]

With-off axis illumination, the angle between the 0 and +1 (or -1) diffraction orders can be increased beyond θ_m, allowing information about finer patterns to be transmitted through the project lens to the image. [1]

h) The bending equation for the deflection $v(x)$ of a buckled beam that is pinned at both ends and subject to a compressive axial end load P is:

$$EI\frac{d^2v}{dx^2} = -Pv$$

where E is Young's modulus and I is the second moment of area. The general solution is of the form:

$$v = A\cos\kappa x + B\sin\kappa x \quad , \quad \kappa = \sqrt{P/(EI)}$$

The boundary conditions are $v = 0$ at $x = 0$ and $x = L$, from which it follows that $A = 0$ and $\kappa = n\pi/L$. The lowest order solution, where $n = 1$, is the only one that occurs in practice, and for this solution we have $\kappa = \pi/L$. The end load on the buckled beam, which is also the critical load for buckling, is therefore:

$$P = EI\kappa^2 = \frac{\pi^2 EI}{L^2}$$

[4]

Solution 4

a) Four process steps are required including the final metallization:

- Photolithography to define pattern in mechanical layer
- Deep reactive ion etching to transfer pattern into mechanical layer
- Sacrificial oxide etch (liquid or vapour phase) to release moving parts
- Gold evaporation

The perforations are required to enable the sacrificial etchant to reach the oxide buried beneath the proof mass. Without them the anchors would be completely undercut before the proof mass was released. [6]

b) With an upward acceleration a, the inertial load on each cantilever will be equivalent to a point load of $-ma/2$ acting at the centre of mass of the proof mass. The bending moment will therefore be:

$$M(x) = -\frac{ma}{2}(l + L/2 - x) \qquad [4]$$

where x is distance along the cantilever measured from the root.

The bending equation is: $$\frac{d^2v}{dx^2} = \frac{M}{EI} = -\frac{6ma}{Ewh^3}(l + L/2 - x) \qquad [4]$$

where $v(x)$ is the deflection profile, E is Young's modulus and $I = wh^3/12$ is the second moment of area of the cantilever. Integrating once, the slope of the deflection profile is obtained as:

$$v'(x) = \frac{dv}{dx} = -\frac{6ma}{Ewh^3}\left[(l + L/2)x - x^2/2\right]$$

Integrating a second time the deflection profile is found to be:

$$v(x) = -\frac{6ma}{Ewh^3}\left[(l + L/2)x^2/2 - x^3/6\right] \qquad [4]$$

The constant of integration was zero in both of the above steps since $v(0) = v'(0) = 0$.

Substituting $x = l$ into the above equations, the deflection and slope at the end of the cantilever are obtained as:

$$v_l = -\frac{l^2(4l + 3L)}{2Ewh^3}ma \quad ; \quad v'_l = -\frac{3l(l + L)}{Ewh^3}ma \qquad [2]$$

c) The baseline capacitance is that of a parallel plate capacitor, i.e. $C_0 = A\varepsilon_0 / g$. With $A = 1$ mm^2 and $g = 2$ μm, this gives $C_0 = 4.427$ pF. Corrections due to the perforations and the cantilevers/anchors have been ignored. [2]

Under applied acceleration the capacitor will become wedge-shaped as the cantilever deflects up or down. Putting $l = 0.3$ mm, $L = 1.0$ mm, $m = 0.96\rho Ah = 2.237 \times 10^{-8}$ kg (factor 0.96 to account for perforations), $w = 20$ μm, $h = 10$ μm, and $a = 10$ ms^{-2}, the cantilever end

deflection and slope are found to be $v_l = -13$ nm, $v'_l = -8.2 \times 10^{-5}$. In this case the capacitance will be that of a wedged air capacitor with the following parameters:

max gap:	$g_2 = g + v_l = 1.987$ μm
min gap:	$g_1 = g_2 + v'_l \times L = 1.905$ μm
wedge angle:	$\theta = -v'_l = 82$ μrad
Capacitor width:	$W = 1$ mm

Subsituting these values into the given formula for a wedged air capacitor, the capacitance at $a = 10$ ms^{-2} is found to be $C = 4.55$ pF. The shift in capacitance is therefore $\Delta C = +0.123$ pF. [4]

The equivalent calculation for $a = -10$ ms^{-2} gives $C = 4.31$ pF. The shift in capacitance in this case is therefore $\Delta C = -0.117$ pF. [2]

The device is non-linear, as can be seen from the fact that the capacitance shifts for $a = \pm 10$ ms^{-2} are not equal and opposite. Non-linearity is to be expected since the capacitance varies with gap according to an inverse square law. [2]

Solution 5

a) In a piezoelectric material, applied stress will generate dielectric polarization and hence surface charge. This is the direct piezoelectric effect. A given stress component may generate polarisation in more than one axis, and the general relationship between the stress and the polarisation is of the form:

$$P_i = d_{ij}\sigma_j$$

where d_{ij} is a 3 x 6 matrix of piezoelectric coefficients. (In the presence of electric field the above equation will also include a normal dielectric response term.) The effect is reversible, so an applied electric field will generate mechanical strain. The direct effect is used for transduction, while the inverse effect is used for actuation. The piezoelectric effect is observed only in non-centrosymmetric crystals, so silicon is not piezoelectric.

In a piezoresistive material, applied stress leads to a change in electrical resistivity. In general both the resistivity and the piezoresistive response will be anisotropic, and the generalised relation between electric field $\boldsymbol{E}$ and current density $\boldsymbol{J}$ is of the form:

$$\boldsymbol{E} = (\rho_0 + \boldsymbol{\Pi}\cdot\boldsymbol{\sigma})\cdot\boldsymbol{J}$$

where ρ_0, $\boldsymbol{\Pi}$ and $\boldsymbol{\sigma}$ are all tensors. Usually symmetries allow these equations to be vastly simplified. [6]

b) To find the relationship between the stress components in the <110>- and <100>-based coordinate frames, we consider the equilibrium of small prismatic elements:

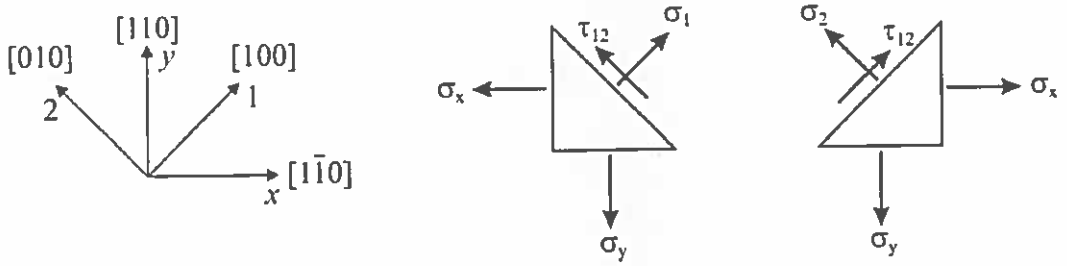

[4]

Resolving forces along [100] in the middle diagram (taking into account the relative lengths of the different sides) gives:

$$\sigma_1\cdot\sqrt{2}a = \sigma_x a\cdot\cos(\pi/4) + \sigma_y a\cdot\cos(\pi/4) \quad\Rightarrow\quad \sigma_1 = \frac{\sigma_x+\sigma_y}{2}$$

Similarly, resolving along [010] in the middle and RH diagrams gives:

$$\tau_{12} = \frac{\sigma_y-\sigma_x}{2} \text{ and } \sigma_2 = \frac{\sigma_x+\sigma_y}{2}.$$ [4]

To relate the axial stress components σ_x and σ_y to each other we need to consider the Generalised Hooke's law relations:

$$E\varepsilon_x = \sigma_x - \upsilon\sigma_y - \upsilon\sigma_z \quad ; \quad E\varepsilon_y = \sigma_y - \upsilon\sigma_z - \upsilon\sigma_x \quad ; \quad E\varepsilon_z = \sigma_z - \upsilon\sigma_x - \upsilon\sigma_y$$

For a membrane in the x-y plane we can assume $\sigma_z = 0$. Also, at a membrane edge aligned to the x-direction, the substrate will prevent expansion along x, implying $\varepsilon_x = 0$. With these two conditions, the first of the Hooke's law relations reduces to:

$$\sigma_x = \upsilon\sigma_y$$ [4]

c) We can assume that the device is aligned to the axes drawn above, so that the piezoresistor lies along the [010] direction. In this case the applied voltage V_{BA} will give rise to an electric field component $E_2 = V_{BA}/l$ and a current along the piezoresistor with density $J_2 = V_{BA}/(l\rho_e)$. In the second equation we have, as instructed, ignored the effects of membrane stress on the longitudinal resistance (the σ_1 and σ_2 terms in the second piezoresistive equation - see *Information for Candidates*). [4]

If the membrane is stressed then, according to the first piezoresistive equation, the shear stress τ_{12} will cause cross-coupling between J_2 and E_1, giving rise to an electric field component $E_1 = \rho_e J_2 \pi_{44} \tau_{12} = \pi_{44} \tau_{12} V_{BA}/l$. This will result in an open-circuit voltage across the piezoresistor of $V_{CD} = wE_1 = \pi_{44} \tau_{12} V_{BA}(w/l)$.

The piezoresistor is located at a position of maximum stress on the membrane, so we know (see *Information for Candidates*) that:

$$\sigma_y = \sigma_{\max} \approx 0.3\frac{pL^2}{h^2}$$

Using this result and the results from Part b), the shear stress τ_{12} can be expressed as:

$$\tau_{12} = \frac{\sigma_y - \sigma_x}{2} = \frac{1}{2}(1-\upsilon)\sigma_y \approx \frac{3}{20}(1-\upsilon)\left(\frac{L}{h}\right)^2 p$$

Substituting for τ_{12} in the expression for V_{CD}, and dividing through by p, the required expression for the sensitivity is obtained. [4]

d) The sensing element is more compact than for a bridge-type sensor which requires 4 piezoresistors. If a bridge is constructed at one position on the membrane then it is not possible for all 4 resistors to be placed at the position of maximum stress and this compromises sensitivity. The 4 resistors can alternatively be placed on different edges of the membrane, but then issues with mis-matching between the resistors (which leads to offset errors) are more likely. [4]

